Estimation of Missing Information in Magnetic Resonance Imaging

Jennifer Salguero Lopez

Universidad Nacional de Colombia
Facultad de Medicina, Departamento de Imágenes Diagnósticas
Bogotá, Colombia
2018

Estimación de información faltante en imágenes de Resonancia Magnética

Jennifer Salguero López

Tesis o trabajo de grado presentada(o) como requisito parcial para optar al título de:
Magister en Ingeniería Biomédica

Director:
Título(MD-M.Sc.-Ph.D.) Eduardo Romero Castro

Línea de Investigación:
Procesamiento de Imágenes
Grupo de Investigación:
Computer Imaging and Medical Applications Laboratory - CIM@ LAB

Universidad Nacional de Colombia
Facultad de Medicina, Departamento de Imágenes Diagnósticas
Bogotá, Colombia
2018

Acknowledgment

I am particularly grateful to the Professor Eduardo Romero for all the knowledge I received during this time, for his patience, effort, dedication and passion in the development of his work and especially for his valuable friendship. I also thank Professor Nelson Velasco for being my guide in this work, for all the time dedicated to transmitting his knowledge and for the immense love he has for this research topic. I would like to thank all the members of the Cimalab research group of the Universidad Nacional de Colombia who contributed their ideas to the development of this research and also to the Gidam research group of Universidad Militar Nueva Granada, with whom I made great friendships. Finally a special thanks to my family and friends who accompanied me in this process.

Abstract

Las fuentes de ruído en resonancia magnética son múltiples y variadas, los artefactos por movimiento y la limitación espacial del captor constituyen las más conocidas. El problema mejor documentado es el denominado volúmen parcial que consiste en que por la limitación espacial del captor, el límite entre dos tejidos distintos se almacena como una señal ponderada enre los dos tejidos [3].Las técnicas de diagnóstico médico han variado en los últimos años, una de las más usadas son las imágenes radiológicas debido a su fácil adquisición y la suficiente información que contienen del tejido estudiado , sin embargo los protocolos de adquisición son limitados y las imágenes obtenidas pierden información importante para el diagnóstico [12]. Estas deficiencias en la adquisición de la información limita al radiólogo y perjudica el diagnóstico y estudio de algunas enfermedades [46].

La resonancia magnética (RM) se usa ampliamente en la medicina hoy en día, pero una desventaja importante es la cantidad de artefactos que afectan la imagen durante el proceso de adquisición. Por ejemplo la resonancia magnética cardíaca (CMR) requiere la sincronización con el ECG para corregir muchos tipos de ruido. Sin embargo, el complejo movimiento del corazón con frecuencia produce cortes desplazados que deben ignorarse o corregirse manualmente ya que la corrección de ECG es inútil en este caso. Este trabajo presenta, entre otros, una metodología novedosa que detecta los artefactos de movimiento en la CMR utilizando un método de prominencia que resalta la región donde se ubican las cámaras del corazón. Una vez que se establece la Región de interés (RdI), su centro de gravedad se determina para el conjunto de cortes que componen el volumen. La desviación del centro de gravedad es una estimación de la coherencia entre los cortes y se utiliza para descubrir los cortes con cierto desplazamiento.

Otra imágen radiológica que también se ve afectada por pérdida de información, son las imágenes de resonancia magnética por difusión, ampliamente utilizadas para estudiar la arquitectura de la materia y comprender sus cambios. La resolución espacial de la imagen ponderada por difusión cerebral (DWI, por sus siglas en inglés) está limitada debido a la alta frecuencia de la imagen y las estructuras cerebrales como bordes o bifurcaciones cuando se capturan los datos. En este enfoque, la idea principal es mejorar la resolución espacial mediante una estrategia de aprendizaje de diccionario y, de este modo, utilizar la dependencia estadística entre diferentes gradientes de la misma imagen para que mejore la resolución. En el siguiente trabajo se realizaron diferentes validaciones para la detección automática de anormalidades haciendo uso de estimadores probabilísticos, todo ello para tener como resultado la detección automática de anormalidades y el incremento de resolución en diferentes modalidades de imágenes médicas.

Palabras clave: pérdida de información, Resonancia magnética, artefactos por movi-

miento, Super-Resolución, SVD. .

Abstract

The sources of noise in magnetic resonance are multiple and varied, the artifacts by movement and the spatial limitation of the captor are the best known. The best documented problem is the so-called partial volume, which consists of the fact that due to the spatial limitation of the captor, the limit between two different tissues is stored as a weighted signal between the two tissues.[3]. Medical diagnostic techniques have changed in recent years, one of the most widely used are radiological images due to its easy acquisition and sufficient information contained in the tissue studied, however the acquisition protocols are limited and the images obtained lose information important for diagnosis [12]. These deficiencies in the acquisition of information limits the radiologist and impairs the diagnosis and study of some diseases [46].

Magnetic resonance imaging (MRI) is widely used in medicine nowadays, yet a significant disadvantage is the amount of artifacts that affect the image during the acquisition process. As an example, Cardiac Magnetic Resonance (CMR) requires synchronization with the ECG to correct many types of noise. However, the complex heart motion frequently produces displaced slices that have to be either ignored or manually corrected since the ECG correction is useless in this case. This work presents a novel methodology that detects the motion artifacts in CMR using a saliency method that highlights the region where the heart chambers are located. Once the Region of Interest (RoI) is set, its center of gravity is determined for the set of slices composing the volume. The deviation of the gravity center is an estimation of the coherence between the slices and is used to find out slices with certain displacement.

Another type of acquisition technique that is affected by the missing information is the Diffusion imaging (dMRI) is a magnetic resonance technique widely used to study the withe matter architecture and to understand their changes. The spatial resolution of brain diffusion weighted imaging (DWI) is limited due to high frequency of the image and brain structures like edges or bifurcations when the data are captured. In this approach the main idea is improved the spatial resolution using a dictionary learning strategy and for this way use the statistical dependence between different gradients of the same image for create a prior that improve the resolution. In the present work it has been different validation methods in order to made automatic detection and the increase resolution of abnormalities using probabilistic information estimation of the medical images.
Keywords: Missing information, Magnetic Resonance Images, motion artifacts, Super-Resolution algorithm Singular Value Decomposition.

Content

List of Symbols, Images and Tables

Symbols with Latin letters

Symbol	Terminus	Unity IS	Definition
D_h	high-resolution dictionary		
D_l	low-resolution dictionary		
t	Time	s	DF
U_j	Low-resolution image		
Y_j	High-resolution image		

Symbols with Greek letters

Symbol	Terminus	Unity IS	Definition
ς	variability for each voxel	1	$\|\|A \cdot V\|\|$
φ_{j}	variability estimated within the same voxel for slice j	1	$\sum_{i=1}^{2} \varsigma_{j,i}$
ϵ	Variability estimated	1	$\frac{\sum_{i=r}^{k} U \cdot S}{\sum_{i=1}^{k} U \cdot S}$

Abbreviations

Abbreviation	Terminus
$2D$	Two-dimensional
$3D$	Three-dimensional
$CUBRIC$	Cardiff University Brain Research Imaging Center
CMR	Cardiac Magnetic Resonance

Abreviations	Terminus
$dMRI$	diffussion of Magnetic Resonance Imaging
DWI	Diffussion-Wighted Image
ECG	Electrocardiogram
FA	Fractional Anisotropy
GC	Gravity Centers
MD	Mean Diffusivity
MR	Magnetic Resonance
MRI	Magnetic Resonance Imaging
MSM	Motion Saliency Map
$OASIS$	Open Access Series of Imaging Studies
OMP	Orthogonal Matching Pursuit
ROI	Region Of Interest
SR	Super-Resolution
SVD	Singular Value Decomposition

List of Images

List of Tables

1 Introduction

Magnetic resonance is an imaging technique that uses the magnetic properties of matter to obtain detailed images of tissues and structures inside the human body. The magnetic resonance images are captured when the radiation is reflected from the body, that is to say that the body is magnetically stimulated so that the radiation is generated in the body, this signal is captured and interpreted by different methods [6]. There are different acquisition techniques such as Diffussion-weighted Image (DWI), where the distribution of gray intensities depends on the diffusion of water in the tissue, which provides great details of functional and anatomical information that can be used in the differential diagnosis of pathological conditions. [50] [12].

The signal acquired in magnetic resonance images and its different modalities can be affected by different types of missing information, such as hardware limitations, patient movements or internal tissues or magnetic susceptibility among others. [35]. Figure **??** shows how the missing information in magnetic resonance images can affect the image in different ways, in this section 3 different forms will be presented, how they are produced and works related to the subject.

1.1. Information Affected by Sources of Movement

The particular effects of movement during capture represent a significant problem since the image is totally or partially distorted by altered contrast or the appearance of so-called echoes or ghosts [52]. Automatic detection of artifacts is a problem attractive due to the low signal-to-noise ratios that are obtained when any of the different artifacts is present. In addition, a detection strategy is obviously the first step of any correction strategy.

In practice, artifact detection is performed directly during the acquisition by the technician who determines the level of distortion of the image and decides, if necessary, to carry out another acquisition. Generally, this technician estimates the level of distortion of the acquired data and determines if the effects of present artifacts can be eliminated or reduced or if the image should be discarded. In this sense, some authors have introduced strategies that quantify or at least compare the levels of distortion between images to include criteria for

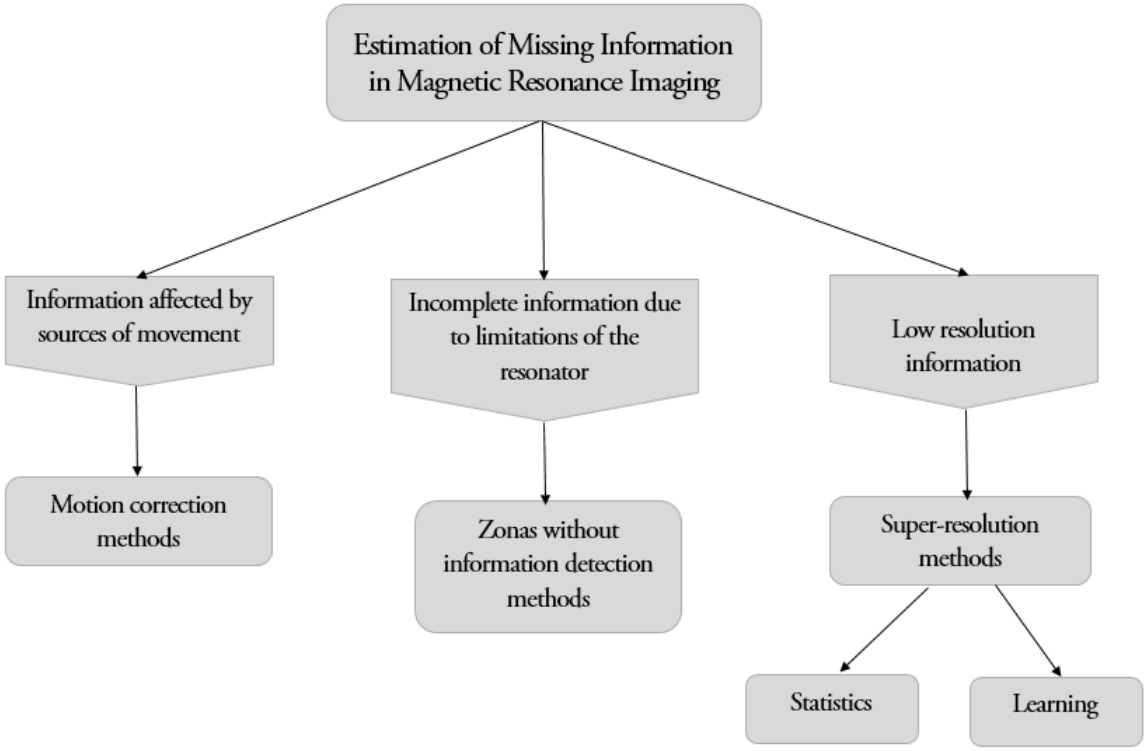

Figure 1-1: Summary of Related Works

discarding objectives in the acquisition protocols.

Super-Resolution (SR) approaches have many advantages for cardiac imaging, these methods provide high resolution images and an understanding of the anatomy and complex function in congenital heart diseases. However, the image damaged by the movement of the patient is a problem in SR approaches. In [42] the authors mention how image misalignment affects the performance of multiple image super resolution strategies.

Other approaches have been used to detect and correct the misalignment in IRM cinema, in [51] the authors introduce a method of reconstruction by patch to exploit the geometric similarities in the space-time domain, [4] the authors used a rigid register of body image in the axial plane to align the position of the fetal heart. Finally, in [8] the authors relied on a register of the local phase to correct the misalignment, in this approach long and short axis cuts are combined.

1.2. Incomplete Information Due to Limitations of the Resonator

Other commonly observed artifacts are those related to the magnetic susceptibility caused by the presence of ferromagnetic and diamagnetic elements that generate a variation of the static magnetic fields and severely affect the image quality. [52, 14, 10]

1.2.1. Low Resolution Information

The study of diffusion images in several places has been used more and more to analyze brain disorders, such as Alzheimer's disease, Huntington's disease and schizophrenia. However, the variability between sites and between scanners of the acquired data poses a potential problem for the joint analysis of MRI diffusion data (dMRI) [55]. This inter-site (or inter-scanner) variability in measurements can come from several sources, including the number of coils used (16- or 32-channel head coil), the sensitivity of the coils, the non-linearity of the image gradient, the homogeneity of the magnetic field, the differences in the algorithms used to reconstruct the data, as well as the changes made during the software updates and other factors related to the scanner. [24]

In different works the resolution has been treated as a Sparse representation theme, that is, with little information to reconstruct the complete image, for this there are two main approaches: the first evaluates statistical methods to increase the resolution and the second creates algorithms by learning of machine to recover lost information. For the first approach there are several works, in [49], the authors use joint information of different gradients in diffusion images to estimate a better reconstruction of the image, this type of approaches that use information from neighborhoods is quite common [29] [47] [7], other authors such as [33] [37] [53] [39] have used techniques such as creation of hosted dictionaries to increase the resolution spatial of the images.

The second approach in super-resolution methods is using pattern training methods and image patches, the authors create models based on patch dictionaries to learn the distribution of information, in [18] [40] [48] the authors use convolved neural networks to pass an image of low spatial resolution to a high resolution, the purposes are different for each approach as a classification of a disease, create more reliable dictionaries among other objectives.

2 Automatic Detection of Perturbed Magnetic Resonance Signal

Presented on the 12th Ïnternational Symposium on Medical Information Processing and Analysis"SIPAIM 2016, November 2016

Magnetic resonance imaging (MRI) is widely used in medicine nowadays, yet a significant disadvantage is the amount of artifacts that affect the image during the acquisition process. This paper presents a strategy for automatic damage detection when the image is altered by movement or there is a loss of information due to magnetic susceptibility. This approach uses a conventional SVD to detect the variability between slices of the image and a region of damaged voxels within the volume. Using a simple derivative algorithm, the method was tested in several cases automatically revealing the distortionâ^{TM}s location with a performance of 74 % for slice damage and 55 % for the volume's damaged region.

2.1. Introduction

Magnetic Resonance Imaging (MRI) is currently the reference in many different medical treatments. The MRI signal capture may be affected by different types of noise such as hardware limitations, physiological motion of patient or organs, or magnetic susceptibility among others [35]. The particular effects of motion during the capture represent a significant problem as the image is total or partially distorted by altered contrast or the appearance of the so called " echoes or ghostlike " [52]. Other artifacts commonly observed are those related with the magnetic susceptibility caused by the presence of ferromagnetic and diamagnetic elements which generate a variation of the static magnetic fields and severely involve the image quality [52, 14, 10]. Automatic detection of artifacts is an appealing problem because of the low signal to noise ratios obtained when any of these noises is present. Additionally, a detection strategy is obviously the first step of any correction strategy. Metallic materials may be present during a MRI capture because the patient has previous treatments with implants, surgical clips, dental fillings or surgical pins that create a distortion of the acquired image. It is acknowledged that main distortions derived from metallic objects appear as black zones where simple data are missing, in very few cases they look as displaced and/or blurred intensities [27].

In practice, the detection of artifacts is performed directly during the acquisition by the technician who determines the image distortion level and decides, if necessary, to carry out another acquisition. Usually, this technician estimates the corruption level of the acquired data and determines whether artifact effects can be eliminated or reduced or if the image must be discarded. In that sense some authors have introduced strategies that quantify or at least compare distortion levels between images, at least to include objective discarding criteria in the acquisition protocols. For example, some authors have analyzed 3D volumes corrupted in some slices by random rotations and translations. These cases are then rigidly registered to quantify how much damage is estimated within the stack of images when compared with a high resolution stack[30, 16, 19]. In [17], fetal MRI brain and surrounding tissues are manually selected to construct a reference stack and the corresponding regions from other stacks may then be located by matching against this reference. The parameters of the rigid transformations between stacks are then used as an objective quantification of the relative location and orientation of each slice. Likewise, a recently developed technique identifies the amount of distortion in a given volume by using a singular value decomposition (SVD) of the volume, with the Frobenius norm as the measure of the likeness between the original volume and its singular decomposition [15]. These authors established a metric for determining the least corrupted image along several stacks of images.

The present approach automatically detects two particular situations for which the Magnetic Resonance signal is perturbed, specifically misplaced acquisitions or rotated slices and distortions caused by magnetic susceptibility. These two cases are solved by linearly decomposing the whole volume using a conventional SVD. If a slice is rotated the data inconsistency is discovered by the SVD decomposition. If a particular region of the volume is not acquired, as is the case of magnetic interferences, this defect is detected by the projection of the signal to the SVD space in different resolutions. The correlation between different scales allows to highlight the specific slices in which

the abnormality occurs.

2.2. Materials and Methods

The principle supporting this method is that there is an inevitable statistical dependence of the spatial information, i.e. two neighbor voxels have a high probability of being alike. This makes any perturbation produces different effects in the data structure that can be detected by searching self-similarity patterns within data. In particular, the data projection to linear spaces is a first order approximation that can be used to search different patterns of inconsistencies. Single Value Decomposition is herein used as a linear model that approximates the data complexity into a first order within which abnormal patterns are sought. The proposed method is able to determine the damaged or distorted regions by any artifact in a series of parallel 2D MRI. The following subsections describe main steps.

2.2.1. Matrix decomposition to obtain orthogonal projections of first order.

The input to the proposed algorithm is a 3D volume composed by series of k 2D parallel slices. Intensity values are organized as a matrix A where each row corresponds to a slice from the original volume. This matrix is the input to the singular value decomposition (SVD) algorithm.

The SVD is a method that linearly represents the data variance of vectors arranged in a usually non-squared matrix. Provided these data are distributed within a subspace with the A matrix dimensions, SVD constructs the representation bases of the data for the different data dimensions, namely the two A dimensions, number of rows and columns. In practice, given the matrix A it can be decomposed into a kind of quadratic form with 3 matrices U, S and V, where S is a diagonal matrix of positive singular values listed in descending order and corresponding to the gains of A when projecting a vector onto U and V. The columns of U and V are orthonormal vectors which can be regarded as bases whose importance depends on the particular singular value, i.e. the largest the singular value the largest the variability along that corresponding axis. Explicitly, a SVD decomposition is given by $A = U \times S \times V^T$.

The variability caused by artifacts in a MR image is therefore detected by two different strategies. The first strategy aims to detect changes affecting a complete slice, the second strategy is focused in detecting damages in a particular volume neighborhood.

2.2.2. Measuring variability among slices

The proposed method looks for a relation between the singular values and the variability presented in an image distorted by MR artifacts. When any distortion is present in the slices of the image, the variability can be associated to the base U and the degree of the variability itself is given by

the eigenvalues of S. In this case the matrix U represents the set of bases of slices, that is to say this matrix has the dimensionality of the number of slices. The variability can be estimated as

$$\varepsilon = \frac{\sum_{i=r}^{k} U \cdot S}{\sum_{i=1}^{k} U \cdot S} \tag{2-1}$$

where ε is the variability estimated within slices of the image, k is the total of columns of the product $U \cdot S$, and r is a threshold value. In this case r has been set to 50, representing the 40 % of slices of the volume approximately.

2.2.3. Measuring variability within stack neighborhoods

When any distortion is present in a region of voxels with different types of noise, the acquisition of these voxels is missed and they appear as small black patches. The associated matrix for voxel variability is V, so the amount of variability for each voxel projected onto the basis V is given by the product:

$$\varsigma = ||A \cdot V|| \tag{2-2}$$

To obtain a representative value of this variability, the two columns of ς are considered because them contains the highest variability

$$\varphi_j = \sum_{i=1}^{2} \varsigma_{j,i} \tag{2-3}$$

φ contains the variability estimated within the same voxel for slice j, taking into account the first two columns is possible to estimate how variable are the intensities along slices.

2.2.4. Automatic detection of MRI artifacts

Automatic detection of an affected region is carried out by approximating the central difference for the second derivative of the estimated variability. Afterwards, the location of specific perturbed slices are automatically recognized using a Threshold detection algorithm. The Eq.2-4 shows the second derivative of ε for the variability among slices. In case of variability within stack neighborhoods, the second derivative must be applied after calculating a weight function, where each φ obtained from the multiresolution method has an associated weight depending on the corresponding level of detail.

$$\triangle 1(n) = \varepsilon(k+1) - 2 * \varepsilon(k) + \varepsilon(k-1) \tag{2-4}$$

$$\triangle 2(n) = \varphi(k+1) - 2 * \varphi(k) + \varphi(k-1) \tag{2-5}$$

2.3. Experimentation and Results

For implementing the proposed method it was used actual brain scans taken from the Open Access Series of Imaging Studies (OASIS) data base [23]. Every scan is composed by a volume of 128 slices and each one of those slices consists in 256x256 intensity. For testing the operation of the method for different artifacts, two tests was performed (see Figure. **2-1**). The first one shows the sensitivity of the approach under different distortion degrees of some slices of the volume. The second one determines the sensitivity of the method under damage in a set of voxels inside the volume.

2.3.1. Detecting rotated slices

The method will first be tested in artifacts which affect slices of the image. In this particular case a rotation is applied on the plane of the image for ten randomly chosen slices. The rotation angle for each slice is chosen randomly between -15 and 15 degrees; the main matrix' dimensions are 128x16384, where rows represent the image's slices and columns represent the corresponding intensities. Once data is organized the SVD is applied to the final matrix and by means of the Eq. 2-1 the estimated variability of the slices is found.

Using Eq. 2-4 to find noticeable changes in variability, a threshold can be established to automatically obtain damaged slices. In order to check the sensitivity and specificity of this approach, the method was probed with 25100 different experiments, for each of which different rotation angles were performed on different slices. To visualize the variability within each slice, the Figure. **2-1** shows the volumes' slice-by-slice variability and its differences when compared to a volume without damage. Table.**2-1** presents method performance for detection of damage present in slices. The sensitivity of 74,4 % indicates the amount of slices with damage detected which correspond to true positives, a notable result when considering the high amount of test cases (25100) affected by several types of damage such as differences in the number of modified (damaged) slices and their rotation angles. Since each image possesses a different range of intensities, one must consider that said intensities can frequently generate high variability between slices, which SVD will incorrectly identify as an error.

2.3.2. Detecting locally affected regions

In order to simulate the damage caused by the magnetic susceptibility in an image, a set of voxels from the image were taken. In this particular case, intensity information for 10 slices of 50*10 pixels each was distorted. By means of the multiresolution analysis a more precise approximation of the damage's location can be obtained. As shown in Figure **2-3** the volume was sliced in quarters to magnify sectional damage, enabling its location by SVD: after applying SVD for each partition, equations 2-2 and 2-3 are used to generate a difference in values obtained for affected versus non-affected zones in each slice, as appreciated in Figure **2-4**. After acquiring said partition values levels are weighted, the deepest one (16×16 pixels) corresponding to the greatest significance in evaluating the complete volume. Calculating the sum of each partition with its corresponding predecessors and applying equation 2-4, the zone where damaged slices have been identified is obtained. The test

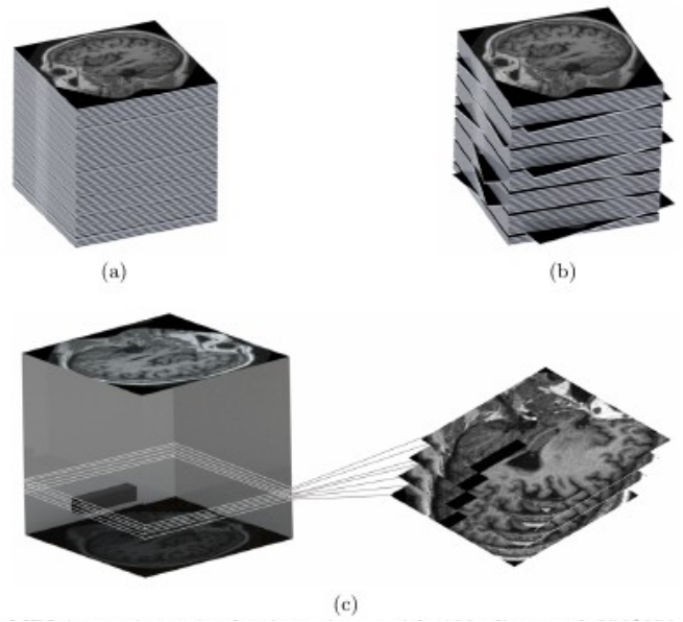

Figure 2-1: Comparison of a volume with rotated slices versus a volume without damage,(a) illustrates the non-damaged volume's variability after SVD application, (b) illustrates the damaged volume's variability after decomposition. One can observe pronounced differences in variability are noticeable when an artifact has taken place.

was performed for 1236 experiments varying the location of the damaged voxel to a different zone within the volume. Table **2-2** presents the performance metrics when evaluating the method when there is a damaged voxel within a volume. Taking into account that for each test case the portion of the volume corresponding to the brain is different, a sensitivity of 0.5479 indicates considerable performance, given that certain cases demonstrate high displacement of the important portion's location and consequently the damaged voxel falls within a high variability zone for which SVD's automatic detection does not function properly. The specificity in this experiment is significant since the method suitably differentiates regions without damage; in future work in image reconstruction this difference can be used to correct specific regions.

Table 2-1: Performance metrics for detection of slices affected by artifacts. Presented values correspond to 25100 different test cases

	Average	Variance	Std.Dev.
Sensitivity	0.7445	0.0103	0.1019
Specificity	0.9199	0.0003	0.0163
Accuracy	0.9037	0.0006	0.0241

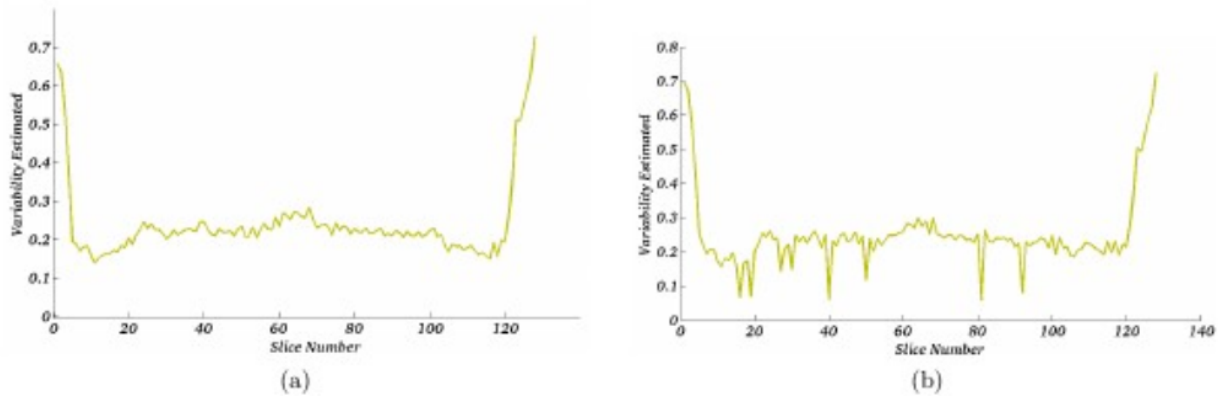

Figure 2-2: Comparison of a volume with rotated slices versus a volume without damage,(2-2a) illustrates the non-damaged volume's variability after SVD application, (2-2b) illustrates the damaged volume's variability after decomposition. One can observe pronounced differences in variability are noticeable when an artifact has taken place.

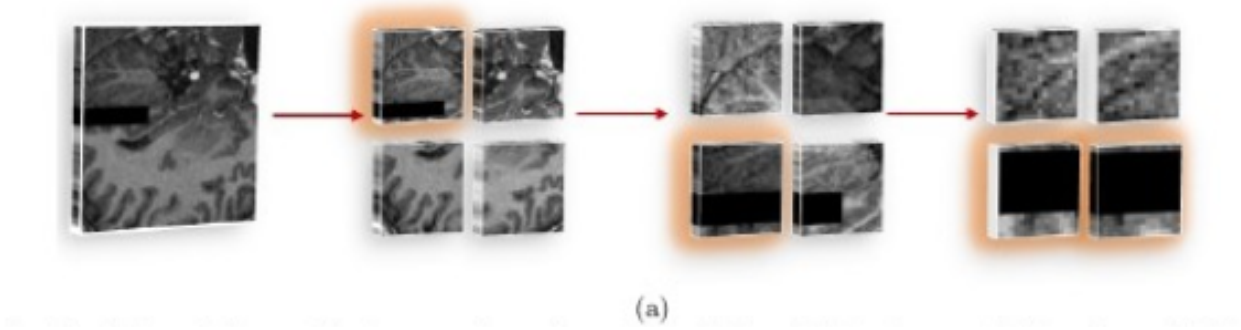

Figure 2-3: The leftmost image displays a volume's portion which exhibits damage in the slices. Each subsequent highlighted level represents a quarter of the previous level. The rightmost image corresponds to the greatest level depth (16×16 pixels) where damage is most noticeable and the method can pinpoint the damage's precise location.

2.4. Conclusions and discussion

This chapter presents a method useful for detecting magnetic resonance signal disturbances generated during the capture process. In particular, detected situations correspond to two different types: inconsistencies in slice alignment (specifically rotated slices) and regions of the volume in which data is missing due to magnetic field interferences.

In this work two types of experimental methods were performed, each one oriented to detecting different information damage. To detect slice misalignment, the SVD was performed in 25100 experiments encompassing a wide variety of damage possibilities in order to expose the coherence

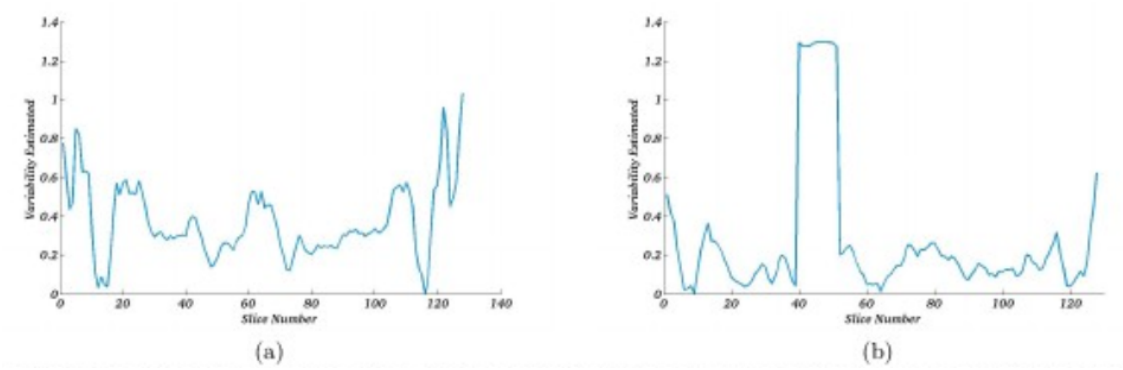

Figure 2-4: Comparison of a volume with a damaged voxel versus a volume without damage,(2-4a) is the variability estimated at the deepest level without damage,(2-4b) presents the same quarter as (2-4a), however in this case there is a damaged voxel in slices 40 to 51.

Table 2-2: Performance metrics for detection of voxel damage. Presented values correspond to 1236 different test cases

	Average	Variance	Std.dev.
Sensitivity	0.5479	0.079	0.281
Specificity	0.9974	0.0002	0.0127
Accuracy	0.9503	0.0009	0.0292

among slices. These experiments indicate considerable performance in artifact detection, although the difficulty of discriminating damage in an image is dependent on the range of intensities and the variability between slices. A sensitivity of 74,45 % indicates that this approach is a promising method to automatically detect and localize corrupted data. When voxel damage is located within a volume, the method' corresponding sensitivity of 54,79 % demonstrates favorable results, taking into account that the method is able to detect a region of $(16 \times 16 \times 10)$ with damage and discriminate regions without damage. In this sense a reconstruction algorithm can be used afterwards to recover lost data or diminish the undesired effects of distortions.

3 Detection of Cardiac MR Images Artifacts Produced by Intrinsic Heart Motion Using a Saliency Mode

Presented on the 13th Ïnternational Symposium on Medical Information Processing and Analysis"SIPAIM 2017, November 2017

*Cardiovascular Magnetic Resonance Imaging is a widely used technique to detect anomalies, evaluate proper function, among others. This imaging technique is susceptible to degradation due to noise and acquisition distortions. Shift motion artifacts are a common distortion due to continuous movement of the heart. This work presents a method to correct this kind of distortions based on the coherence information estimation between two or more images acquired with different plane orientations. To estimate the information coherence a metric is calculated using the intensity values of voxels, after which the correction can be achieved using an optimization strategy. To evaluate the proposed method misalignment was simulated with both artificial images and Cardiac Resonance Images, the results are similar for the two tests taking into account that the movement in slice plane was of 1 to 5 pixels in two directions (X and Y). Misaligment in the resulting image after applying the method was minimal (*0,26 *pixels in* X *direction and* 0,32 *pixels in* Y *direction).*

3.1. Introduction

Cardiovascular Magnetic Resonance Imaging allows evaluation of heart diseases. Different characteristics may be observable, namely the anatomical heart structure, the blood pool, the papillary muscles and their relation with the heart valves, among others. However, the capturing process demands considerable periods of time since this examination requires synchronization with respect to the cardiac cycle by electrocardiography (ECG).[54, 41] Despite this synchronization, the long acquisition periods facilitate contamination with different types of noise. Overall, motion artifacts result inevitable in heart images by the high complex dynamics. Essentially, the heart efficiency depends on two types of complementary movements: a rotation around the short-axis and a twisting motion along the long axis. During the cardiac cycle the base rotates clockwise during systole while the apex rotates counterclockwise, a torsion effect that powers the blood out the left ventricle[36, 25]. In addition, the acquisition protocol suggests the patient must remain breathe-hold for periods of some seconds. This mixture of random movements make displacement between slices a frequent artifact in cardiac MRI.

In practice, these artifacts or misalignments are commonly found in cine MRI[52]. Detection and correction of these artifacts is a later step. Some authors in consequence have introduced strategies that quantify the distortion level to correct this artifact. In [34] We demonstrated how the information incoherence can be used to detect alterations or artifacts in magnetic resonance images although this incoherence worked with MRI of brain, for cardiac MRI case, it is not enough due the low-resolution of the Cardiac cine images and the significant changes between frames hence many approaches are fixed the goal to improve the image quality and remove the artifacts reconstructing the complete image, with different approaches (e.g. super-resolution techniques[42, 43], Adaptive patch-based reconstruction, among others[51, 2]), these approaches have a limitation with motion artifacts, these methods does not work when there are big misalignment between slices hence the early detection of misalignment slices are very important before a super-resolution approach.

Likewise, a recently developed technique identifies the amount of misalignment of the slices with the final goal of corrected the image and make a three-dimensional reconstruction, for this case, the authors use the intersection lines between slices with the combination of short axes and long axes images, the cross-correlation of local phases give a spatial coherence that is used to find the misalignment and corrected it,due that this method works with different axes acquisition is necessary to have the axes to detect the motion in the image that which is a great disadvantage [44].

A main contribution of the present approach is a fully automated detection of inconsistencies during the capturing process. Specifically, inter-slice misalignment produced by motion in cardiac MRI. This type of artifact is common during the acquisition process and eventually can misled heart measurements performed by experts. The method starts by detecting the region of interest (ROI), where the cardiac chambers are located, by a a saliency approach. Afterwards, the region is binarized by a conventional isodata approach and the cardiac chambers are delimited. The center of gravity of these chambers is slice-per-slice set. A consistency analysis consists then in establishing how far is any individual centroid from the trajectory described by the whole set of centroids. Any

misalignment is automatically detected since centroids usually are located at the same distance of the inter-centroid trajectory.

3.2. Materials and Methods

The aim of this work was to automatically detect displaced heart slices that may occur in short-axis cardiac MRI. The underlying hypothesis is that cardiac heart is a continuous structure and therefore must keep certain coherence between the consecutive slices, i.e., abrupt shape changes are not observed between consecutive slices. The method can be summarized as follows: a first step is a coarse detection of the region where the heart is located, as previously described in [5]. A conventional isodata approach delineates the cardiac chambers and their center of gravity is computed for every slice in the volume. Finally, a minimum squared distance sets the best trajectory that approximates the whole set of centroids, any misalignment is usually an outlier of this curve along the stack.

3.2.1. Heart detection along the slice stack

A first task consists in finding the region where the heart is located, slice per slice. Assuming that heart is the only object moving in cine MRI, motion saliency map (MSM) is computed.
A saliency map mimics the human visual system since local features are salient when there is a certain contrast with their surroundings. Motion changes are estimated for every smoothed image I at a particular location δ. Taking into account that one slice δ at the time t changes with respect to rest of the frames, the Δ stores these differences between the image I_t at the time t and the image I_k at any other time k. Once these differences are calculated, a grid of patches p (5 x 5 pixels) is superimposed to each σ and the entropy H is calculated to every patch p. Higher entropies represent more motion and therefore, higher saliency. The MSM is defined as

$$MSM(\delta)_{t,p} = \sum_{k=1}^{N} H(|\Delta_t(\sigma_{t,p})|) \tag{3-1}$$

3.2.2. Binarizing the ROI

In this step a binary 2D ROI enclosing the heart is obtained for each slice. A threshold is then applied to the MSM and the ROI is delineated. The isodata algorithm [28] identifies the complete location of the cardiac chambers. (Figure:**??**, center panel).

3.2.3. Measuring distance between gravity centers

Once a ROI is automatically set, the next step is to calculate the trajectory conformed by the gravity centers (GC) of the whole volume, typically 8 to 15 slice centroids. Specifically, this curve is approximated with a linear regression by minimizing the slice centroid distance to a line along the heart structure in the basal-to-apex direction. Any misalignment is then detected by setting the

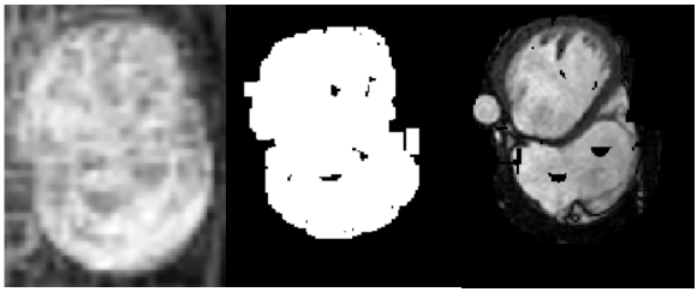

Figure 3-1: Coarse heart localization. The left panel displays the obtained MSM, the center panel shows the binarized MSM, and the right panel shows the final ROI superimposed with the original image.

possible distance outliers. Figure:**??** shows the different slices of a heart volume at the diastole time of the cardiac cycle. The slice gravity center, in red, is drawn together with the line of centroids, in blue. Observe how the misaligned slice (third panel from left to right in the bottom row) shows the two points far apart.

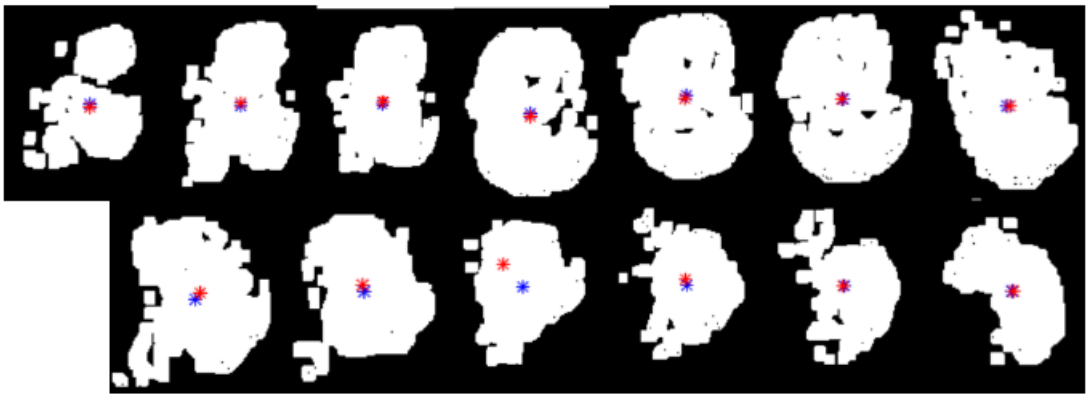

Figure 3-2: Each of the panels corresponds to the coarse heart localization after binarization. The slice gravity center (in red) and the curve of centroids (in blue) are drawn together. Third panel from left to right at the bottom row shows how these two points are far when a misalignment by motion occurs.

3.2.4. Automatic detection of misalignment

A misalignment is automatically detected by a threshold of the second derivative of the distance ∇ between the gravity centers (the Euclidean distance d) as follows

$$\bigtriangledown = d_{(k+1)} - 2(d_k) + d_{(k-1)} \tag{3-2}$$

3.3. Experimentation and Results

Quantitative experiments were performed using artificial misalignments in real images of cardiac cine MRI. The used data set was composed of five CMR cases acquired in a $1{,}5\,T$ scanner from five different subjects. The used cases are composed of a variable number of series (between 8 to 14 series), Each series containing between 8 to 15 slices and an inter-slice separation varying between 8 in-plane resolution of 256×256 and a pixel spacing of $1{,}8\,mm$. The proposed method was proved in two scenarios, the first with simulated misalignments and the second with real misalignment.

3.3.1. Detecting simulated misalignment slices

To simulate misalignment artifacts, the slice plane was displaced in X and Y axes. In this part of the evaluation, 4 cases serve to perform 100 experiments with a random slice misalignment that varied between 4 to 8 pixels.

Figure **3-3** shows the distance of gravity centers when there exists misalignments, red circle plots the distance when no misalignments are present while green square illustrates how this metrics is altered if a slice id displaced.
Table **3-1**. shows the quantitative results for whole set of experiments.

Table 3-1: Performance metrics for detecting slice displacement. Presented values corresponds to 100 different experiments per case and 4 different cases

	Average ± Std Dev
Recall	0.84 ± 0.11
Fscore	0.68 ± 0.13
Precision	0.59 ± 0.10

3.3.2. Detecting real misaligned slices

The proposed method was evaluated with 2 cases with real misalignments, as illustrated in figure **3-4** and figure **3-5**.

3.4. Conclusions and discussion

This chapter presents a method to detect displacement in Cardiac Magnetic Resonance generated during the capture process. The approach detect misalignment of a slice in a volume, this distortion is very common in this type of image due to the way (breath-hold) acquisition and the long time

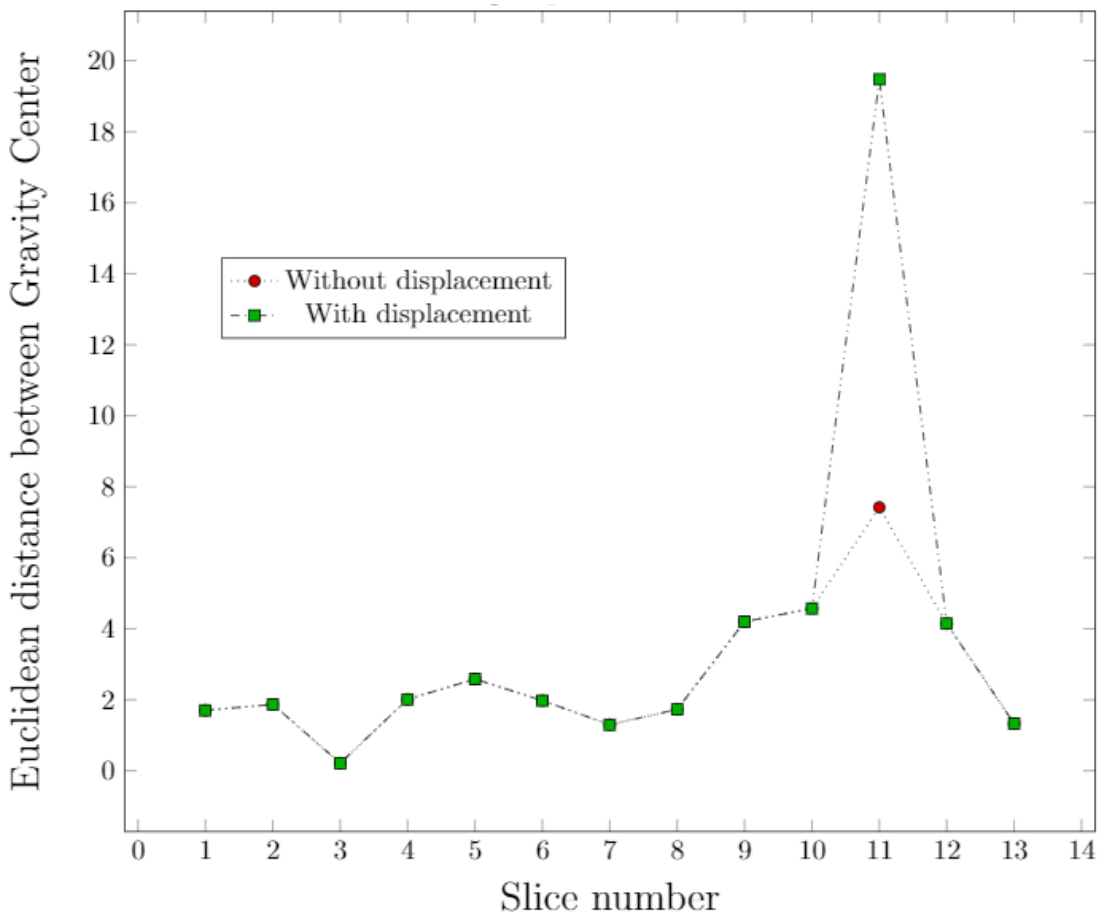

Figure 3-3: Comparison of a volume with misaligned slices (green square) versus a volume without displacement (red circle). Observe how the metric is altered in right panel.

required.

The presented method is based on the shape coherence of the cardiac chambers through the volume, each slice in an image corresponding to one part of heart, by structural coherence is feasible to suppose that the gravity center of heart is an axis that cross the whole volume, when the center of gravity of a slice is far of this axis, it is possible to determine that the slice has a displacement.

As part of the method a motion saliency map and an image binarization strategies were used [5]. Combination of this techniques demonstrate its applicability in an artifact detection use. We consider that application exploration of this strategy have to be performed in future work.

The measuring of distances between local (slice) GC and global (volume) GC demonstrated its value to determine the misalignment. Authors consider that this approach can be used as a metric (measure of the misalignment degree) into a future work oriented to misalignment correction algorithms.

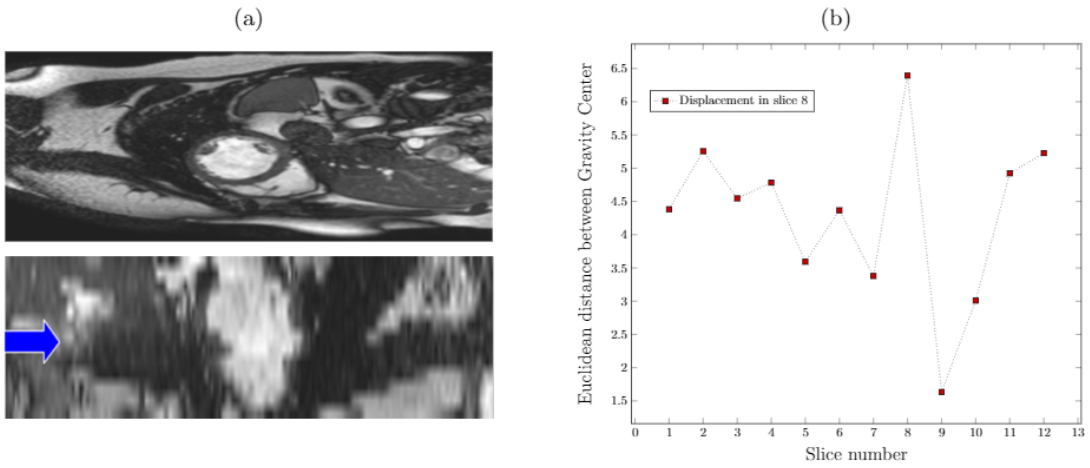

Figure 3-4: The proposal method applied in two real misalignments, in both cases the detection was correct

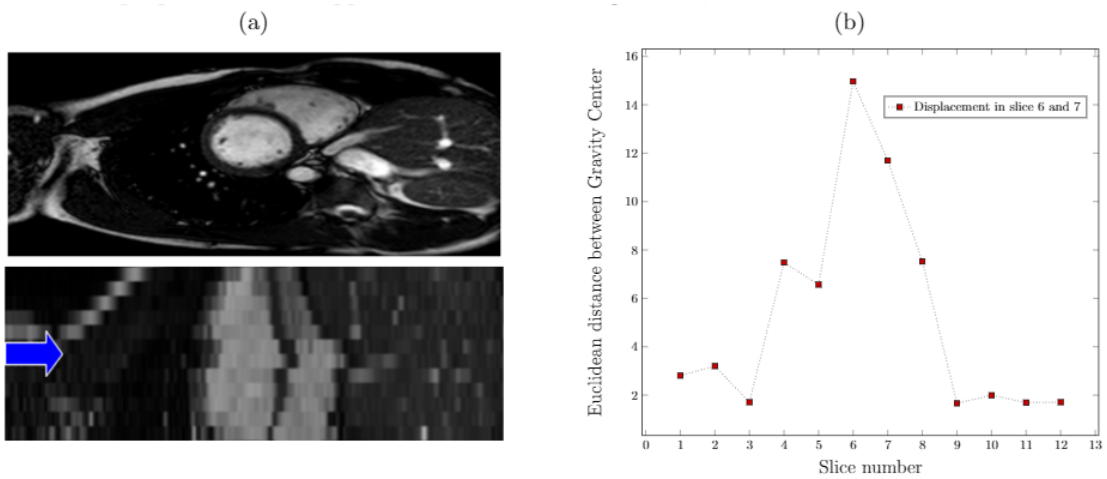

Figure 3-5: The proposal method applied in two real misalignments, in both cases the detection was correct

4 Super-Resolution for Diffusion Magnetic Resonance Imaging using gradients' dependencies

4.1. Introduction

Diffusion-weighted imaging (DWI) is a magnetic resonance imaging technique which measures the random water motion (diffusion) in tissues. The diffusion process is affected by natural barriers such as neuronal membranes in white matter, the effect on diffusion is observed using measures like fractional anisotropy (FA), mean diffusivity (MD)and other which are directly calculated from image data [45], other way to represent the diffusion process is using a predefined model of the diffusion, the most widely used is the diffusion tensor model. All methods applied to that allows highlights micro-organization of the white matter for posterior analysis[20, 13]. The white matter is examined to study and diagnose some neurodegenerative illness, for this reason, is necessary a big quantity of images from several radiological centers and high spatial resolution for each image. These last reasons represent a problem for the experts and the resonance centers due to the variability of the acquisition machine producing an image with a different source of noise, different and bad resolution and finally uncomparable images as a result.

4.1.1. Super-resolution and sparse representation in diffusion images

Different image analysis approaches have presented many methods in order to increase the resolution of Magnetic Resonance images, some of them decompose the images in some semantic atoms from the brain tissue, that allows constructing semantic-based dictionaries from brain MR images. [33]

Super-Resolution (SR) techniques have been broadly used to increasing medical image resolution [9]. At the beginning, these methods attempted to recover a high-resolution image by combining multiple shifted low-resolution acquisitions. Two kinds of approaches can be identified: one works at the acquisition level over raw data (frequency space), while the others act on the volumetric images (spatial or image space) as an additional processing step. At the acquisition stage, the k-space data can be manipulated and combined to obtain adequate spatial resolution while reducing acquisition time [11]; or parameters can be configured to obtain multiple scans with different slice directions which are then mixed up [38, 33]. Recent approaches have changed the classical SR paradigm with multiple images, evolving towards the use of information from a single low-resolution image, but

also improving the image information by combining different modalities. Patch-based approaches with non-local regularization frameworks have been proposed by [31] and [7], which have also extended the formulation to super-resolve low-resolution T2w images using high-frequency information from T1w images ([32]; [22]).

Different image analysis approaches, such as non-negative matrix factorization [21] or sparse and redundant representations [26], use this assumption at their very base. These two methods, in particular, identify the constituent parts of a scene and then, using some of them, the same scene or similar ones may be accurately reconstructed. These parts, denoted as basis functions or atoms, are usually arranged in overcomplete dictionaries with a larger number of elements than the effective dimensionality of the input space, thereby representing a wider range of image phenomena.[33]

4.2. Proposed Methodology

The proposed method consists of two different construction of the dictionaries, the high-resolution dictionary is constructed using the different gradients of each diffusion image for the same patient. Then the low-resolution dictionary is obtained by sub-sampling the high-resolution dictionary. In order to find the sparse representation of the images set, it was used the local dependencies to each gradient to obtain prior information to recover high frequencies in the image patches. The K-SVD algorithm obtains the bases with a higher variance that represents the original image creating a dictionary with a sparse base. Finally using both dictionaries the patch-based spatial super-resolution is obtained.

4.2.1. Dictionary construction

The high-resolution dictionary construction was initialized using a set of high-resolution image Y_j and the corresponding low-resolution image was the down-sampling and blurred image from Y_j, U_j. Our approach creates two different dictionaries over complete, the high-resolution dictionary D_h is constructed by collecting a fixed number of patches at the same image location but in the different gradient image. The low-resolution dictionary is the down-sampling version of D_h, D_l.

In order to obtain the high frequencies that are missed in the image, the present approach uses statistical dependence in the different gradient images per patient, to initialize the dictionary in high resolution was used the original images of the patient, a random gradient was taken as Y_j and the different gradients of the same patch initialized the dictionary D_i show in figure **4-1**.

The initialize dictionary was constructed using a patch size of $6x6x6$ from the information of the complete brain. To obtain the sparse information we used the K-SVD algorithm described by Aharon et al.[1], the main idea is to obtain that of searching the best possible dictionary D for the sparse representation of the training set Y. First, we fix and aim to find the best coefficient matrix X.

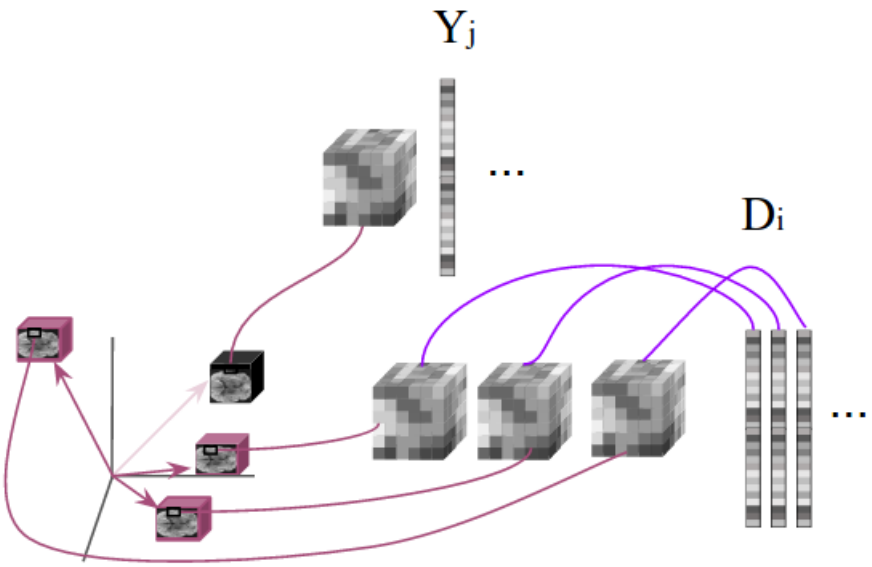

Figure 4-1: Illustration of high-Resolution dictionary initialization

$$\min_{D,X} \left\{ \|Y - DX\|_F^2 \right\} \quad \text{subject to} \quad \forall i, \|x_i\|_0 \leq T_0 \tag{4-1}$$

As finding the truly optimal is impossible as long as it can supply a solution with a fixed and predetermined number of nonzero entries T_0, we use an approximation pursuit method, in this case, we use the *Orthogonal Matching Pursuit (OMP)* algorithm. After that the SVD algorithm finds the closest matrix (in Frobenius norm) that approximates the X and minimize the error between Y and DX, we obtain a new dictionary D with atoms that represent the directions variance.

Finally, the high-resolution dictionary D_h is obtained. Down-sampling D_h we obtain the low-resolution dictionary D_l whereby the number of atoms in the dictionary has not changed.

4.2.2. Local Reconstruction of the high-resolution DW image

Once the dictionaries D_h and D_l are constructed, the next stage is related with the estimation of a high-resolution version given low-resolution image volume Y_l. The reconstruction stage involves two steps: first, a local reconstruction is made for each patch, and then, a global image regularization is performed.

4.3. Experimentation and results

The whole dataset, for both training and validation, is composed of one high resolution DW images, obtained from the Cardiff University Brain Research Imaging Center (Cubric). The DW image is

acquired using a 3T MR General Electric scanner. A standard spin-echo EPI pulse sequence with sensitivity encoding is applied to obtain the DWI data at 30 different diffusion directions, with the following parameters: matrix size: 128 x 128 with 64 slices and spatial resolution of 1.8 x 1.8 x 1.8 mm. The super-resolution method has been implemented using MATLAB R2017a (Mathworks Inc.), run in a Linux PC with Intel Core i5 and 4 GB of RAM.

Table 4-1: Comparison of PSNR and SSIM values achieved with a standard bicubic interpolation, the Manhon et al. reconstruction method and the proposed super-resolution reconstruction.

	Bicubic interpolation	Manhon et al.	Proposed approach
PSNR	36.45	37.23	34.24
SSIM	0.963	0.972	0.834

5 Discussion and conclusion

This work has focused on the study of different medical images modalities in order to know their limitations and how to correct them. The missing information is a normal problem that affects any modality in resonance images hence we center in search of relevant information that allows estimating this information and made an approximation in order to obtain an image with better quality. Three main ideas were proposed in order to carry out the objectives of the research. In the first modality of magnetic resonance, the main idea is to find automatically some perturbed information specifically misplaced acquisitions or rotated slices and distortions caused by magnetic susceptibility, the second approach was the automatic detection of inter-slice misalignment produced by motion in cardiac MRI and the last approach was focus on the increase of resolution in diffusion-weighted magnetic resonance imaging. All the previous approaches show the limitations of the magnetic resonance and how these limitations corrupt the signal.
The first approach that we made in order to find missing information was the classical problem of the magnetic resonance images, the artifacts. This work presents a noise detection method, particularly two different kinds of MRI noise related with patient motion and magnetic susceptibility. As a posterior step, other noise sources can be explored such us a"ghostlike" artifacts or echoes, in that case some adaptations of basic technique proposed must be applied e.g. including a noise prior model to detect it in the decomposition or different partitioning of data before decomposition. Other scenario for promising future work is a work flow oriented to characterize the way information is altered, in that sense, knowledge about statistical differences among characteristics of the affected region and non-affected regions, a reconstruction method can be properly designed to achieve good results.

The second part of this approach was focused in detect some misalignment of the cardiac images. As a part of the method a motion saliency map and an image binarization strategies were used [5]. Combination of this techniques demonstrate its applicability in an artifact detection use. We consider that application exploration of this strategy have to be performed in future work.In a first approximation, it was simulated the misalign with four cases, each one with 100 different experiments with different translation and slice displacement. The performance of this method was of 84 % to detect the correct misalign slice, this result indicates the good performance of the method taking into account that the image have a slice thickness of 8mm approximately in consequence the variation in gravity center could be normal and not to represent a displacement. Then the algorithm discriminate regions without damage and allows a posterior correction e.g. with a simple register method. As a conclusion of this part, We estimated missing information successfully obtained an automatic method that allows to find an image error for a posterior correction.

Bibliografía

[1] Aharon, Michal ; Elad, Michael ; Bruckstein, Alfred [u. a.]: K-SVD: An algorithm for designing overcomplete dictionaries for sparse representation. En: *IEEE Transactions on signal processing* 54 (2006), Nr. 11, p. 4311

[2] Ahmed, Abdul H. ; Qureshi, Ijaz M. ; Shah, Jawad A. ; Zaheer, Muhammad: Motion correction based reconstruction method for compressively sampled cardiac MR imaging. En: *Magnetic Resonance Imaging* 36 (2017), p. 159–166

[3] Alexander, Andrew L. ; Hasan, Khader M. ; Lazar, Mariana ; Tsuruda, Jay S. ; Parker, Dennis L.: Analysis of partial volume effects in diffusion-tensor MRI. En: *Magnetic Resonance in Medicine* 45 (2001), Nr. 5, p. 770–780

[4] van Amerom, Joshua F. ; Lloyd, David F. ; Price, Anthony N. ; Kuklisova Murgasova, Maria ; Aljabar, Paul ; Malik, Shaihan J. ; Lohezic, Maelene ; Rutherford, Mary A. ; Pushparajah, Kuberan ; Razavi, Reza [u. a.]: Fetal cardiac cine imaging using highly accelerated dynamic MRI with retrospective motion correction and outlier rejection. En: *Magnetic Resonance in Medicine* (2017)

[5] Atehortúa, Angélica ; Zuluaga, Maria A. ; García, Juan D. ; Romero, Eduardo: Automatic segmentation of right ventricle in cardiac cine MR images using a saliency analysis. En: *Medical Physics* 43 (2016), Nr. 12, p. 6270–6281

[6] Bushong, Stewart C. ; Clarke, Geoffrey: *Magnetic resonance imaging: physical and biological principles*. Elsevier Health Sciences, 2014

[7] Coupé, Pierrick ; Manjón, José V ; Chamberland, Maxime ; Descoteaux, Maxime ; Hiba, Bassem: Collaborative patch-based super-resolution for diffusion-weighted images. En: *NeuroImage* 83 (2013), p. 245–261

[8] Grau, Vicente: Correction of Slice Misalignment in Multi-breath-hold Cardiac MRI Scans. En: *Statistical Atlases and Computational Models of the Heart. Imaging and Modelling Challenges: 7th International Workshop, STACOM 2016, Held in Conjunction with MICCAI 2016, Athens, Greece, October 17, 2016, Revised Selected Papers* Vol. 10124 Springer, 2017, p. 30

[9] Greenspan, Hayit: Super-resolution in medical imaging. En: *The Computer Journal* 52 (2008), Nr. 1, p. 43–63

[10] Hargreaves, Brian A. ; Worters, Pauline W. ; Pauly, Kim B. ; Pauly, John M. ; Koch, Kevin M. ; Gold, Garry E.: Metal-induced artifacts in MRI. En: *American Journal of*

Roentgenology 197 (2011), Nr. 3, p. 547–555. – ISBN 1546–3141 (Electronic)\r0361–803X (Linking)

[11] Herment, A ; Roullot, E ; Bloch, I ; Jolivet, O ; De Cesare, A ; Frouin, F ; Bittoun, J ; Mousseaux, E: Local reconstruction of stenosed sections of artery using multiple MRA acquisitions. En: *Magnetic Resonance in Medicine: An Official Journal of the International Society for Magnetic Resonance in Medicine* 49 (2003), Nr. 4, p. 731–742

[12] Holdsworth, Samantha J. ; Bammer, Roland: Magnetic resonance imaging techniques: fMRI, DWI, and PWI. En: *Seminars in neurology* Vol. 28 NIH Public Access, 2008, p. 395

[13] Horsfield, Mark A. ; Jones, Derek K.: Applications of diffusion-weighted and diffusion tensor MRI to white matter diseases–a review. En: *NMR in Biomedicine* 15 (2002), Nr. 7-8, p. 570–577

[14] Jarraya, M. ; Hayashi, D. ; Guermazi, A. ; Kwoh, C. K. ; Hannon, M. J. ; Moore, C. E. ; Jakicic, J. M. ; Green, S. M. ; Roemer, F. W.: Susceptibility artifacts detected on 3T MRI of the knee: Frequency, change over time and associations with radiographic findings: Data from the Joints on Glucosamine Study. En: *Osteoarthritis and Cartilage* 22 (2014), Nr. 10, p. 1499–1503. – ISSN 15229653

[15] Kainz, Bernhard ; Steinberger, Markus ; Wein, Wolfgang ; Kuklisova-Murgasova, Maria ; Malamateniou, Christina ; Keraudren, Kevin ; Torsney-Weir, Thomas ; Rutherford, Mary ; Aljabar, Paul ; Hajnal, Joseph V. ; Rueckert, Daniel: Fast Volume Reconstruction from Motion Corrupted Stacks of 2D Slices. En: *IEEE Transactions on Medical Imaging* 34 (2015), Nr. 9, p. 1901–1913. – ISBN 0278–0062

[16] Keraudren, K. ; Kuklisova-Murgasova, M. ; Kyriakopoulou, V. ; Malamateniou, C. ; Rutherford, M. A. ; Kainz, B. ; Hajnal, J. V. ; Rueckert, D.: Automated fetal brain segmentation from 2D MRI slices for motion correction. En: *NeuroImage* 101 (2014), p. 633–643. – ISBN 1095–9572 (Electronic)\r1053–8119 (Linking)

[17] Kim, Kio ; Habas, Piotr A. ; Rousseau, Francois ; Glenn, Orit A. ; Barkovich, Anthony J. ; Studholme, Colin: Intersection based motion correction of multislice MRI for 3-D in utero fetal brain image formation. En: *IEEE Transactions on Medical Imaging* 29 (2010), Nr. 1, p. 146–158. – ISBN 1558–0062 (Electronic)\r0278–0062 (Linking)

[18] Kondo, Yuto ; Han, Xian-Hua ; Chen, Yen-Wei: Two-step learning based super resolution and its application to 3D medical volumes. En: *Consumer Electronics (GCCE), 2015 IEEE 4th Global Conference on* IEEE, 2015, p. 326–327

[19] Kuklisova-Murgasova, Maria ; Quaghebeur, Gerardine ; Rutherford, Mary A. ; Hajnal, Joseph V. ; Schnabel, Julia A.: Reconstruction of fetal brain MRI with intensity matching and complete outlier removal. En: *Medical Image Analysis* 16 (2012), Nr. 8, p. 1550–1564. – ISBN 1361–8415

[20] Lebel, Catherine ; Treit, Sarah ; Beaulieu, Christian: A review of diffusion MRI of typical white matter development from early childhood to young adulthood. En: *NMR in Biomedicine* (2017), p. e3778–n/a. – ISSN 1099–1492

[21] Lee, Daniel D. ; Seung, H S.: Learning the parts of objects by non-negative matrix factorization. En: *Nature* 401 (1999), Nr. 6755, p. 788

[22] Manjón, José V ; Coupé, Pierrick ; Buades, Antonio ; Collins, D L. ; Robles, Montserrat: MRI superresolution using self-similarity and image priors. En: *Journal of Biomedical Imaging* 2010 (2010), p. 17

[23] Marcus, Daniel S. ; Wang, Tracy H. ; Parker, Jamie ; Csernansky, John G. ; Morris, John C. ; Buckner, Randy L.: Open Access Series of Imaging Studies (OASIS): cross-sectional MRI data in young, middle aged, nondemented, and demented older adults. En: *Journal of cognitive neuroscience* 19 (2007), Nr. 9, p. 1498–1507. – ISBN 0898–929X

[24] Mirzaalian, Hengameh ; Ning, Lipeng ; Savadjiev, Peter ; Pasternak, Ofer ; Bouix, Sylvain ; Michailovich, O ; Grant, G ; Marx, CE ; Morey, Rajendra A. ; Flashman, LA [u. a.]: Inter-site and inter-scanner diffusion MRI data harmonization. En: *NeuroImage* 135 (2016), p. 311–323

[25] Nakatani, Satoshi: Left ventricular rotation and twist: why should we learn? En: *Journal of cardiovascular ultrasound* 19 (2011), Nr. 1, p. 1–6

[26] Olshausen, Bruno A. ; Field, David J.: Sparse coding with an overcomplete basis set: A strategy employed by V1? En: *Vision research* 37 (1997), Nr. 23, p. 3311–3325

[27] Panfili, Elisabetta ; Pierdicca, Laura ; Salvolini, Luca ; Imperiale, Luigi ; Dubbini, Jeffrey ; Giovagnoni, Andrea: Magnetic resonance imaging (MRI) artefacts in hip prostheses: a comparison of different prosthetic compositions. En: *La Radiologia medica* 119 (2014), Nr. 2, p. 113–20. – ISSN 1826–6983

[28] Ridler, TW ; Calvard, S [u. a.]: Picture thresholding using an iterative selection method. En: *IEEE trans syst Man Cybern* 8 (1978), Nr. 8, p. 630–632

[29] Robinson, M D. ; Chiu, Stephanie J. ; Lo, J ; Toth, C ; Izatt, J ; Farsiu, Sina: New applications of super-resolution in medical imaging. En: *Super-Resolution Imaging* 2010 (2010), p. 384–412

[30] Rousseau, F ; Glenn, O ; Iordanova, B ; Rodriguez-Carranza, C ; Vigneron, D ; Barkovich, J ; Studholme, C: A novel approach to high resolution fetal brain MR imaging. En: *Medical image computing and computer-assisted intervention : MICCAI ... International Conference on Medical Image Computing and Computer-Assisted Intervention* 8 (2005), Nr. Pt 1, p. 548–55. – ISBN 3540293272

[31] Rousseau, François: Brain hallucination. En: *European Conference on Computer Vision* Springer, 2008, p. 497–508

[32] Rousseau, François ; Initiative, Alzheimerâ^{TM}s Disease N. [u. a.]: A non-local approach for image super-resolution using intermodality priors. En: *Medical image analysis* 14 (2010), Nr. 4, p. 594–605

[33] Rueda, Andrea ; Malpica, Norberto ; Romero, Eduardo: Single-image super-resolution of brain MR images using overcomplete dictionaries. En: *Medical image analysis* 17 (2013), Nr. 1, p. 113–132

[34] Salguero, Jennifer ; Velasco, Nelson ; Romero, Eduardo: Automatic Detection of Perturbed Magnetic Resonance Signal, 2017

[35] Schmidt, Maria A. ; Payne, Geoffrey S.: Radiotherapy planning using MRI. En: *Physics in Medicine and Biology* 60 (2015), Nr. 22, p. R323–R361. – ISBN 0031–9155

[36] Sengupta, PP ; Tajik, AJ ; Chandrasekaran, K ; Khandheria, BK: Twist mechanics of the left ventricle: principles and application. JACC Cardiovasc Imaging. 2008; 1 (3): 366-76 / Epub 2009/04/10. – Informe de Investigación

[37] Shi, Wenzhe ; Caballero, Jose ; Ledig, Christian ; Zhuang, Xiahai ; Bai, Wenjia ; Bhatia, Kanwal ; de Marvao, Antonio M Simoes M. ; Dawes, Tim ; OÂ^{TM}Regan, Declan ; Rueckert, Daniel: Cardiac image super-resolution with global correspondence using multi-atlas patchmatch. En: *International Conference on Medical Image Computing and Computer-Assisted Intervention* Springer, 2013, p. 9–16

[38] Shilling, Richard Z. ; Robbie, Trevor Q. ; Bailloeul, TimothÉe ; Mewes, Klaus ; Mersereau, Russell M. ; Brummer, Marijn E.: A super-resolution framework for 3-D high-resolution and high-contrast imaging using 2-D multislice MRI. En: *IEEE transactions on medical imaging* 28 (2009), Nr. 5, p. 633–644

[39] Tang, Songze ; Guo, Haitao ; Zhou, Nan ; Huang, Lili ; Zhan, Tianming: Coupled dictionary learning on common feature space for medical image super resolution. En: *Image Processing (ICIP), 2016 IEEE International Conference on* IEEE, 2016, p. 574–578

[40] Umehara, Kensuke ; Ota, Junko ; Ishimaru, Naoki ; Ohno, Shunsuke ; Okamoto, Kentaro ; Suzuki, Takanori ; Shirai, Naoki ; Ishida, Takayuki: Super-resolution convolutional neural network for the improvement of the image quality of magnified images in chest radiographs. En: *Medical Imaging 2017: Image Processing* Vol. 10133 International Society for Optics and Photonics, 2017, p. 101331P

[41] Usman, Muhammad ; Atkinson, David ; Odille, Freddy ; Kolbitsch, Christoph ; Vaillant, Ghislain ; Schaeffter, Tobias ; Batchelor, Philip G. ; Prieto, Claudia: Motion corrected compressed sensing for free-breathing dynamic cardiac MRI. En: *Magnetic resonance in medicine* 70 (2013), Nr. 2, p. 504–516

[42] Velasco, Nelson F. ; Rueda, Andrea ; Santa Marta, Cristina ; Romero, Eduardo: A sparse Bayesian representation for super-resolution of cardiac MR images. En: *Magnetic Resonance Imaging* 36 (2017), p. 77–85

[43] Villalon-Reina, Julio E. ; Thompson, Paul M. ; Romero, Eduardo [u. a.]: Bayesian super-resolution in brain diffusion weighted magnetic resonance imaging (DW-MRI). En: *12th International Symposium on Medical Information Processing and Analysis* International Society for Optics and Photonics, 2017, p. 101601J–101601J

[44] Villard, Benjamin ; Zacur, Ernesto ; DallÂ^{TM}Armellina, Erica ; Grau, Vicente: Correction of Slice Misalignment in Multi-breath-hold Cardiac MRI Scans. En: *International Workshop on Statistical Atlases and Computational Models of the Heart* Springer, 2016, p. 30–38

[45] Yang, Edward ; Nucifora, Paolo G. ; Melhem, Elias R.: Diffusion MR imaging: basic principles. En: *Neuroimaging Clinics of North America* 21 (2011), Nr. 1, p. 1–25

[46] Yang, Guang ; Ye, Xujiong ; Slabaugh, Greg ; Keegan, Jennifer ; Mohiaddin, Raad ; Firmin, David: Combined self-learning based single-image super-resolution and dual-tree complex wavelet transform denoising for medical images. En: *Medical Imaging 2016: Image Processing* Vol. 9784 International Society for Optics and Photonics, 2016, p. 97840L

[47] Yang, Jianchao ; Wright, John ; Huang, Thomas S. ; Ma, Yi: Image super-resolution via sparse representation. En: *IEEE transactions on image processing* 19 (2010), Nr. 11, p. 2861–2873

[48] Yang, Xiong ; Zhant, Shu ; Hu, Changsheng ; Liang, Zhicheng ; Xie, Dongdong: Super-resolution of medical image using representation learning. En: *Wireless Communications & Signal Processing (WCSP), 2016 8th International Conference on* IEEE, 2016, p. 1–6

[49] Yang, Zhipeng ; He, Peiyu ; Zhou, Jiliu ; Wu, Xi: Non-local diffusion-weighted image super-resolution using collaborative joint information. En: *Experimental and Therapeutic Medicine* 15 (2015), Nr. 1, p. 217–225

[50] Yao, Xiu-Zhong ; Kuang, Tiantao ; Wu, Li ; Feng, Hao ; Liu, Hao ; Cheng, Wei-Zhong ; Rao, Sheng-Xiang ; Wang, He ; Zeng, Meng-Su: Comparison of diffusion-weighted MRI acquisition techniques for normal pancreas at 3.0 Tesla. En: *Diagnostic and interventional radiology* 20 (2014), Nr. 5, p. 368

[51] Yoon, Huisu ; Kim, Kyung S. ; Kim, Daniel ; Bresler, Yoram ; Ye, Jong C.: Motion adaptive patch-based low-rank approach for compressed sensing cardiac cine MRI. En: *IEEE transactions on medical imaging* 33 (2014), Nr. 11, p. 2069–2085

[52] Zaitsev, Maxim ; Maclaren, Julian ; Herbst, Michael. *Motion artifacts in MRI: A complex problem with many partial solutions.* 2015

[53] Zhang, Jinpeng ; Zhang, Lichi ; Xiang, Lei ; Shao, Yeqin ; Wu, Guorong ; Zhou, Xiaodong ; Shen, Dinggang ; Wang, Qian: Brain atlas fusion from high-thickness diagnostic magnetic resonance images by learning-based super-resolution. En: *Pattern recognition* 63 (2017), p. 531–541

[54] Zhang, Shuo ; Joseph, Arun A. ; Voit, Dirk ; Schaetz, Sebastian ; Merboldt, Klaus-Dietmar ; Unterberg-Buchwald, Christina ; Hennemuth, Anja ; Lotz, Joachim ; Frahm, Jens: Real-time magnetic resonance imaging of cardiac function and flowâ"recent progress. En: *Quantitative imaging in medicine and surgery* 4 (2014), Nr. 5, p. 313–329

[55] Zhu, Tong ; Hu, Rui ; Qiu, Xing ; Taylor, Michael ; Tso, Yuen ; Yiannoutsos, Constantin ; Navia, Bradford ; Mori, Susumu ; Ekholm, Sven ; Schifitto, Giovanni [u. a.]: Quantification of accuracy and precision of multi-center DTI measurements: a diffusion phantom and human brain study. En: *Neuroimage* 56 (2011), Nr. 3, p. 1398–1411